

## Scaling-up Fracture Pore Space Permeability – Approach to Mine Water Inflow Prediction

Eunjeong SEOK<sup>1</sup>, John E. GALE<sup>2</sup>

<sup>1</sup>*Department of Earth Sciences, Memorial University, St. John's, NL, A1A 3E7, Canada, eunjeong\_ffc@nfld.net*

<sup>2</sup>*John E. Gale, Fracflow Consultants Inc., 154 Majors Path, St. John's, NL, A1A 5A1, john\_ffc@nfld.net*

**Abstract** Pore space and permeability data from a fully characterized fracture plane, measured under controlled biaxial shear loading conditions, were used to determine the scaling-up or averaging approach that provided the best match between measured and computed flow-rates. The fracture flow-rates that were computed using average permeability values and randomly assigned aperture values did not match the measured flow-rate. However the computed flow-rate matched well to the measured flow-rate when the permeability values reflected the underlying fracture aperture spatial variability, indicating that spatial structure is a key factor when scaling-up to predict mine water inflows in fractured rock masses.

**Key Words** Fracture permeability, scaling up, laboratory data, spatial variability, predicting flow-rates.

### Introduction

Predictions of mine water inflows in fractured rock masses are based on a small number of borehole packer measurements, one or more aquifer tests and, infrequently, one or more test drift inflow measurements. These borehole and drift measurements generally exhibit a wide range in permeability values and sample a very small part of the rock mass that will contribute to mine inflows. In addition, the local and mine scale structures usually impart a strong anisotropy to the fractured rock mass permeability. The challenge to hydrogeologists is to 'scale-up' from these point measurements to the 3D mine scale when the sampling is incomplete and the boundary conditions are not well defined.

### Permeability and Scale Effect

Permeability data (fig. 1) compiled and interpreted by Clauser (1992), for both porous and fractured media, show that the range of hydraulic properties appears to be about 7 to 8 log scales ( $\text{Log}_{10}$  ranged from -15 to -23 with permeability in  $\text{m}^2$ ) for small laboratory samples, with the range of the permeability values decreasing as the scale of measurement or sample size increases. However, this reduction in range may be related more to a smaller number of samples for sample sizes greater than 10 cm than to an actual narrowing of the range of permeability values.

Measurements at the borehole scale (fig. 1) usually include test sections of the rock mass that are many times larger or orders of magnitude larger than most laboratory samples. Borehole measurements show a much wider range in measured values than is shown by the laboratory data. In addition, the average or mid-range borehole measurements reported by Clauser (1992) are higher than those presented for the laboratory scale samples. Obviously, borehole test sections capture open fractures and discontinuities that are not captured or not well represented in laboratory samples. The regional scale data tabulated by Clauser (1992) are limited in number and each site or area, in most cases, is represented by only one data point.

Overall, there appears to be a trend of increasing permeability with increasing sample size up to the 100 m scale, followed by a poorly defined pattern of decreasing permeability at the regional scale where the interpretation of the permeability values for these large regional aquifer systems is based on measured and assumed boundary conditions. Gale (1993) added additional laboratory data to the data set that was presented by Clauser (1992), for a range of porous and fractured samples, and showed that the range for the permeability of laboratory scale samples could be extended to cover approximately 13 log cycles. Using the mid-range values only, Gale (1993) noted that the borehole and regional scale values fell within the mid range of the permeability values that were determined from laboratory data.

Obviously, part of this change with sample size is contributed by small-scale heterogeneities that become more significant as the size of the sample decreases. In addition, test boundary con-

ditions and the lower measurement limits are much more precisely defined in small-scale laboratory samples and generally much more poorly defined or assumed in borehole tests, with the heterogeneities generally being averaged over significant lengths of the borehole test interval. Changes with sample size are normally refer to as the “scale effect” and considerable effort has been devoted to developing scaling up procedures without fully examining the permeability database from which these scale effects are inferred. For example extensive numerical investigations have been conducted (Margolin et.al., 1998, among others) to determine how key parameters scale with an increase in the area of interest but without the benefit of a fully characterized database to calibrate the model simulations. A fully defined fracture pore space database is used in this paper to compare the computed and measured flow-rates using different averaging and data generation techniques.

**Laboratory Investigations**

The pore space geometry of the laboratory sample that was used in this investigation was fully characterized with well-defined boundary conditions (Seok, 2001). Both flow and tracer tests were completed on a 190 by 290 mm section of a fracture plane, that was subject to a range of normal and shear stresses using a biaxial shear frame. At the final load, and following a final flow and tracer test, a room temperature resin was injected into the fracture plane. Once the resin cured, the fracture planes were sectioned, perpendicular to the plane, and the width (aperture) of each local fracture opening was measured using a photo-microscope and digitizer approach at selected intervals. Analysis of the pore-space data demonstrated that the fracture pore-space geometry, consisting of contact areas and open fracture pore space, is characterized by a bimodal distribution with a well defined spatial structure. Since the pore-space geometry was mapped along discrete sections through the fracture-plane sample, simulated annealing was used to recreate the pore-space geometry over the entire sample area (Seok, 2001). This approach was found to respect both the bimodal nature and the spatial structure of the fracture pore-space geometry. The fracture pore space was generated on a 1 mm grid to capture the spatial variability of the fracture permeability values (fig 2).

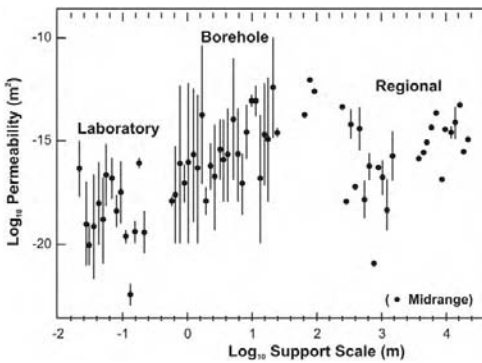


*Figure 1 Permeability of crystalline rocks and characteristic scale of measurements (Clauser, 1992)*

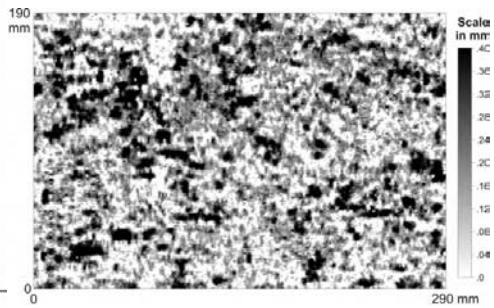


*Figure 2 Pore space map of the annealed data for ASPO2*

In low-permeability fractured rocks, it has been assumed by some investigators that flow and transport are controlled by a number of high-permeability pathways, consisting of or within discrete fractures (Margolin et. al., 1998). However, the pore space map for the fracture plane (fig 2), while it shows zones or pockets of high permeability or large local apertures the pore space map does not show any continuous zones or channels that extend across the fracture plane. Instead the pore space geometry has a well-defined spatial structure as shown by the semi-variogram (fig. 3). Obviously, without adequate deterministic fracture-property databases, it will be difficult to validate the various conceptual models of flow in fracture systems along with the appropriate scaling relationships.

### 3D Model Input Parameters

The measured pore space or aperture data from the simulated annealing process were converted to fracture hydraulic conductivities using the equation for the modified parallel plate model (Seok, 2001), with a relative roughness term,  $e_m/D_H$ , where  $e_m$  is the average surface roughness and  $D_H$  is the hydraulic diameter of the fracture such that for fractures in contact the relative roughness is 0.5. The fracture hydraulic conductivities were converted to equivalent porous medium conductivity and assigned as input parameters in the 3D FEFLOW flow and transport model (Diersch, 2005).  $K_f$  and  $K_m$  are assigned as the conductivities of the fracture plane and the porous media model such that  $K_f \cdot 2b \cdot W = K_m \cdot s \cdot W$ , where  $2b$  is the fracture aperture,  $s$  is the fracture spacing and  $W$  is the width of the fracture and the flow model. Since the hydraulic gradient should be the same between the experimental data and the model, the model equivalent porous media conductivity,  $K_m$ , can be calculated using the fracture conductivity as  $K_m = K_f \cdot (2b/s)$ .

### Assessing Scaling Relationships Using Pore Space Data

As noted above, many mine-water inflow 3D model predictions are based on a small number of borehole permeability measurements and limited or no drift inflow data. Given the sparse nature of the permeability measurements, the underlying structure of the permeability distribution is not known. Generally the average of the borehole permeability measurements, the geometric mean or the harmonic mean or even the arithmetic mean, is used to populate the 3D model with modifications for depth and rock type. In many cases, these data sets are not corrected for truncation and censoring errors. Confidence in the calibration of the 3D model inflow predictions is limited since the actual mine water inflow is not known. Since both the permeability distribution as well as the flow and hydraulic head boundary conditions are fully defined for the flow through this single discrete fracture, we are able to determine how the prediction of the measured fracture flow-rate is affected by the size of the sub-sample from the overall fracture plane. The fracture plane pore-space geometry was divided into 55,100, 1 mm, grid cells. The entire discrete fracture plane was divided into a series of blocks whose size were the selected sample scale. Each block was numbered sequentially. Thirty block numbers were selected from the entire list of blocks using a random number generation for each sample size. This procedure was repeated for each sub-sample. To demonstrate the role of scale, five different sub-sample sizes were used: 10 mm by 10 mm (100 mm<sup>2</sup>; fig. 4), 15 mm by 15 mm (225 mm<sup>2</sup>), 20 mm by 20 mm (400 mm<sup>2</sup>), 30 mm by 30 mm (900 mm<sup>2</sup>) and 40 mm by 40 mm (1600 mm<sup>2</sup>). Figure 4 shows the randomly selected locations for the 10 mm by 10 mm sub-samples. Each group of sub-samples consisted of 30 samples except for the 40 mm by 40 mm samples where only 27 samples were generated due to the size of the original fracture plane.

A 3D flow model was constructed for each of the subsamples with a 1 mm by 1 mm grid size and one model layer. Flow in both the X direction ( $Q_x$ ) and Y direction ( $Q_y$ ), were simulated for each subsample. The injection head was increased proportional to the sample size so that the hydraulic head for each subsample was the same. No-flow boundaries were assigned to two sides of

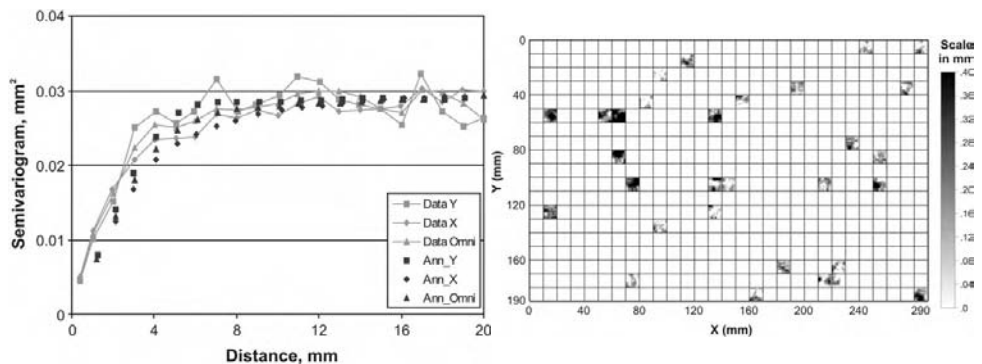


Figure 3 Semivariogram of the annealed data for Figure 4 Sub-sampling at 10 mm scale to simulate flow

the sample and constant head values were assigned to the other two sides. The aperture for each grid cell was used to calculate the hydraulic conductivity for each cell. The computed flow-rate was normalized with respect to the hydraulic head. Then the difference in the model size was normalized by dividing the flux by a ratio of width to 10 mm. Figure 5 shows box plots of normalized flux for  $Q_x$  and  $Q_y$  and aperture. The average and median normalized flux ( $Q^*$ ) values for each group are also plotted. The normalized flux that was measured during the laboratory test is also plotted as a line for comparison.

Comparison of the computed and measured flux showed 1) smaller subsamples had greater variability in computed flux, 2) the computed flux gradually increased with increasing sample size until it converged to the measured flux when the subsample size was 400 mm<sup>2</sup>, 3) the simulated flux based on average permeability values and that based on the randomly assigned values did not match the measured value, 4) the computed flux matched well to the measured flux when the permeabilities were constrained by the underlying spatial variability over the fracture plane.

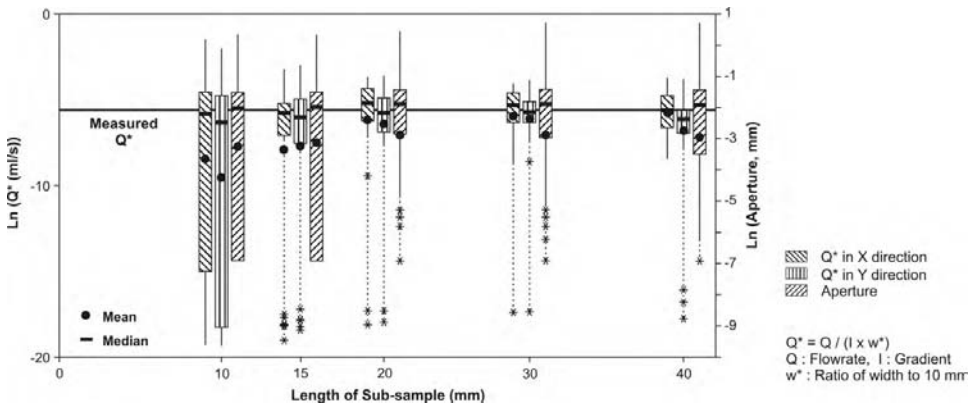


Figure 5 Statistics of the flow-rates for each sub-sample versus sample size

**Conclusions**

These numerical model simulations show that with increasing sample size, the predicted flow-rates rapidly converge on the measured flow-rates. Characterizing the spatial structure of the underlying permeability data is required if one is to successfully predict flow-rates in a given system. Flow-rates, predicted using average and or randomly assigned permeability values to populate the entire model area do not match the measured flow-rates.

**Acknowledgements**

The authors thank Fracflow Consultants Inc. for providing financial support and the fracture pore space data that were used in this investigation.

**References**

Clauser, C. (1992) Permeability of crystalline rocks. EOS, Trans. AGU, 73:21, pp. 233  
 Diersch, H. -J. G. (2005) FEFLOW 5.3 Finite Element Subsurface Flow and Transport Simulation System. WASY GnbH, Institute for Water Resources Planning and Systems Research, Berlin, Germany  
 Gale, J. E. (1993) Fracture properties from laboratory and large scale field tests: Evidence of scale effects. Proceedings of the Second International Workshop on Scale Effects in Rock Masses, Lisbon, Portugal, June 1993, (ISRM), pp. 341 – 352  
 Margolin, Gennady, Brian Berkowitz and Harvey Scher (1998) Structure, flow, and generalized conductivity scaling in fracture networks. Water Resources Research, v. 34, no. 9, pp 2103 – 2121  
 Seok, E. (2001) Pore space characterization and implications for flow simulation in discrete fracture planes. M.Sc. Thesis, Memorial University of Newfoundland, Canada, 166 p  
 Seok, E. (2010) Impact of Variability in Laboratory and Field Fracture Permeability Data on Simulated Flux as a Function of Scale and Spatial Structure, PhD. Thesis, Department of Earth Sciences, Memorial University of Newfoundland, St. John’s, NL, Canada, (In-progress)